

Second-Order Eikonal Corrections for $A(e, e'p)$

B. Van Overmeire, J. Ryckebusch

*Department of Subatomic and Radiation Physics, Ghent University,
Proeftuinstraat 86, B-9000 Gent, Belgium*

Abstract

The first-order eikonal approximation is frequently adopted in interpreting the results of $A(e, e'p)$ measurements. Glauber calculations, for example, typically adopt the first-order eikonal approximation. We present an extension of the relativistic eikonal approach to $A(e, e'p)$ which accounts for second-order eikonal corrections. The numerical calculations are performed within the relativistic optical model eikonal approximation. The nuclear transparency results indicate that the effect of the second-order eikonal corrections is rather modest, even at $Q^2 \approx 0.2$ (GeV/c)². The same applies to polarization observables, left-right asymmetries, and differential cross sections at low missing momenta. At high missing momenta, however, the second-order eikonal corrections are significant and bring the calculations in closer agreement with the data and/or the exact results from models adopting partial-wave expansions.

Key words: $A(e, e'p)$ reactions, eikonal approximation, second-order corrections, optical potentials

PACS: 11.80.Fv, 24.10.Ht, 24.10.Jv, 25.30.Dh

1 Introduction

The eikonal approximation [1–3] has a long history of successful results in describing scattering processes like nucleon-nucleus scattering, heavy-ion collisions, and electroinduced nucleon-knockout reactions. The latter class of reactions, usually denoted as $A(e, e'p)$, provide access to a wide range of nuclear phenomena like short- and long-range correlations, relativistic effects, the transition from hadronic to partonic degrees of freedom, and medium modifications of nucleon properties. The interpretation of $A(e, e'p)$ data heavily relies on an

Email address: Jan.Ryckebusch@UGent.be (J. Ryckebusch).

accurate description of the effect of the final-state interactions (FSI), i.e., the interactions of the ejected proton with the residual nucleus such as rescattering and/or absorption. The eikonal approximation has been widely used to treat these distortions, either in combination with optical potentials [4–7], or with Glauber theory, its multiple-scattering extension [8–15].

The eikonal scattering wave functions are derived by linearizing the continuum wave equation for the ejected proton. Hence, the solution is only valid to first order in $1/k$, with k the proton’s momentum, and the eikonal approximation is suited for the description of reactions at sufficiently high energies. To extend the applicability to lower energies, Wallace [16] has developed systematic corrections to the eikonal scattering amplitude. Several authors have investigated the effect of higher-order eikonal corrections in elastic nuclear scattering by protons, antiprotons, and α particles [17, 18], heavy-ion collisions [19–22], and inclusive electron-nucleus scattering [23]. The aim of this Letter is to determine the influence of higher-order eikonal corrections on $A(e, e'p)$ observables. To this purpose, we extend the relativistic optical model eikonal approximation (ROMEIA) $A(e, e'p)$ framework of Ref. [7]. Our formalism builds upon the work of Baker [24], where an eikonal approximation for potential scattering was derived to second order in $1/k$. Here, this work is extended to include the effect of the spin-orbit potential.

The outline of this Letter is as follows. In Section 2, the second-order eikonal correction to the ROMEIA model is derived. Section 3 presents the results of the $A(e, e'p)$ numerical calculations. We look into how the second-order eikonal correction affects more inclusive quantities like the nuclear transparency, as well as truly exclusive observables such as the induced normal polarization P_n , the left-right asymmetry A_{LT} , and the differential cross section. Finally, in Section 4, we state our conclusions.

2 Formalism

For the description of the $A(e, e'p)$ reaction, we adopt the impulse approximation (IA) and the independent-nucleon picture. Within this approach, the basic quantity to be computed is the transition matrix element [25]

$$\langle J^\mu \rangle = \int d\vec{r} \bar{\Psi}_{\vec{k}, m_s}^{(-)}(\vec{r}) \hat{J}^\mu(\vec{r}) e^{i\vec{q}\cdot\vec{r}} \phi_{\alpha_1}(\vec{r}). \quad (1)$$

Here, ϕ_{α_1} and $\Psi_{\vec{k}, m_s}^{(-)}$ are the relativistic bound-state and scattering wave functions, with α_1 the quantum numbers of the struck proton and \vec{k} and m_s the momentum and spin of the ejected proton. The relativistic bound-state wave

function is obtained in the Hartree approximation to the $\sigma - \omega$ model [26] with the W1 parametrization for the different field strengths [27]. The scattering wave function $\Psi_{\vec{k}, m_s}^{(-)}$ appears with incoming boundary conditions and is related to $\Psi_{\vec{k}, m_s}^{(+)}$ by time reversal. Furthermore, \hat{J}^μ is the relativistic one-body current operator. Throughout this Letter, we use the Coulomb gauge and the CC2 form of \hat{J}^μ [28].

We now turn our attention to the determination of the scattering wave function $\Psi_{\vec{k}, m_s}^{(+)}$. We start by considering the Dirac equation for a proton with relativistic energy $E = \sqrt{k^2 + M_N^2}$ and spin state $|\frac{1}{2}m_s\rangle$ subject to Lorentz scalar and vector potentials $V_s(r)$ and $V_v(r)$. The Dirac equation for the four-component spinor $\Psi_{\vec{k}, m_s}^{(+)}(\vec{r})$ is converted to a Schrödinger-like equation for the upper component $u_{\vec{k}, m_s}^{(+)}(\vec{r})$ [7, 29]

$$\left[-\frac{\nabla^2}{2M_N} + V_c(r) + V_{so}(r) (\vec{\sigma} \cdot \vec{L} - i\vec{r} \cdot \hat{\vec{p}}) \right] u_{\vec{k}, m_s}^{(+)}(\vec{r}) = \frac{k^2}{2M_N} u_{\vec{k}, m_s}^{(+)}(\vec{r}) . \quad (2)$$

The central $V_c(r)$ and spin-orbit $V_{so}(r)$ potentials are defined in terms of the scalar and vector ones, $V_s(r)$ and $V_v(r)$. The lower component $w_{\vec{k}, m_s}^{(+)}(\vec{r})$ is related to the upper one through

$$w_{\vec{k}, m_s}^{(+)}(\vec{r}) = \frac{1}{E + M_N + V_s(r) - V_v(r)} \vec{\sigma} \cdot \hat{\vec{p}} u_{\vec{k}, m_s}^{(+)}(\vec{r}) . \quad (3)$$

When solving Eq. (2) in the eikonal approximation, a standard procedure is to replace the momentum operator $\hat{\vec{p}}$ by the asymptotic momentum \vec{k} in the spin-orbit ($V_{so}(r) \vec{\sigma} \cdot \vec{L}$) and Darwin ($V_{so}(r) (-i\vec{r} \cdot \hat{\vec{p}})$) terms, as well as in the lower component (3). In literature, this is usually referred to as the effective momentum approximation (EMA) [30]. For the upper component, one puts forward a solution of the form

$$u_{\vec{k}, m_s}^{(+)}(\vec{r}) \equiv N \eta(\vec{r}) e^{i\vec{k} \cdot \vec{r}} \chi_{\frac{1}{2}m_s} , \quad (4)$$

i.e., a plane wave modulated by an eikonal factor $\eta(\vec{r})$. Here, N is a normalization factor.

In the ROMEA approach [7, 29], which adopts the first-order eikonal approximation, Eq. (2) is linearized in $\hat{\vec{p}}$ leading to a solution for the eikonal factor of the form

$$\eta^{\text{ROMEA}}(\vec{r}) = \eta^{\text{ROMEA}}(\vec{b}, z) = \exp \left(-i \frac{M_N}{k} \int_{-\infty}^z dz' V_{\text{opt}}(\vec{b}, z') \right) , \quad (5)$$

where $\vec{r} \equiv (\vec{b}, z)$, the z axis lies along the momentum \vec{k} of the proton, and $V_{\text{opt}}(\vec{b}, z) = V_c(\vec{b}, z) + V_{so}(\vec{b}, z) (\vec{\sigma} \cdot \vec{b} \times \vec{k} - ikz)$. Despite the fact that it is written as an exponential phase, the solution (5) is only valid up to first order in V_{opt}/k .

In what follows, we will derive an expression for the eikonal factor $\eta(\vec{r})$ that is valid up to order V_{opt}/k^2 . The momentum dependence in the spin-orbit and Darwin terms makes that these terms are retained up to order V_{so}/k , while central terms are included up to order V_c/k^2 . Note that the expansion is not expressed in terms of the Lorentz scalar and vector potentials V_s and V_v . Looking for a solution of the form (4) for the Schrödinger-like equation (2), Baker arrived at the following equation for the eikonal factor (see Eq. (14) of Ref. [24]):

$$\begin{aligned} \eta(\vec{b}, z) = & 1 - i \frac{M_N}{k} \int_{-\infty}^z dz' V_{\text{opt}}(\vec{b}, z') \eta(\vec{b}, z') + \frac{M_N}{2k^2} V_{\text{opt}}(\vec{b}, z) \eta(\vec{b}, z) \\ & + \frac{M_N}{2k^2} \int_{-\infty}^z dz' (z - z') \left(\frac{1}{b} + \frac{\partial}{\partial b} \right) \frac{\partial}{\partial b} \left(V_{\text{opt}}(\vec{b}, z') \eta(\vec{b}, z') \right). \quad (6) \end{aligned}$$

Note that, apart from dropping contributions of order V_{opt}/k^3 and higher, no additional assumptions were made when deriving Eq. (6). In Ref. [24], Eq. (6) was subsequently solved for spherically symmetric potentials. The spin-orbit and Darwin terms, however, break the spherical symmetry and a novel method to solve Eq. (6) is needed. To that purpose, we assume that the derivative of the function η is of higher order in $1/k$ than η itself (as is true for the ROMEA solution (5)). This allows us to drop the $\partial\eta/\partial b$ contribution in the last term of Eq. (6), as it is of order V_{opt}/k^3 or higher:

$$\begin{aligned} & \frac{M_N}{2k^2} \int_{-\infty}^z dz' (z - z') \left(\frac{1}{b} + \frac{\partial}{\partial b} \right) \frac{\partial}{\partial b} \left(V_{\text{opt}}(\vec{b}, z') \eta(\vec{b}, z') \right) \\ & = \frac{M_N}{2k^2} \left(\frac{1}{b} + \frac{\partial}{\partial b} \right) \int_{-\infty}^z dz' (z - z') \\ & \quad \times \left[\frac{\partial}{\partial b} \left(V_c(\vec{b}, z') + V_{so}(\vec{b}, z') (\vec{\sigma} \cdot \vec{b} \times \vec{k} - ikz') \right) \right] \eta(\vec{b}, z'). \quad (7) \end{aligned}$$

Spherical symmetry implies that $z' \partial V_c(\vec{b}, z')/\partial b = b \partial V_c(\vec{b}, z')/\partial z'$. Hence, the $z' \partial V_c/\partial b$ term in Eq. (7) can be written as

$$\begin{aligned}
& -\frac{M_N}{2k^2} \left(\frac{1}{b} + \frac{\partial}{\partial b} \right) \int_{-\infty}^z dz' b \frac{\partial V_c(\vec{b}, z')}{\partial z'} \eta(\vec{b}, z') \\
& = -\frac{M_N}{2k^2} \left(\frac{1}{b} + \frac{\partial}{\partial b} \right) \int_{-\infty}^z dz' b \frac{\partial}{\partial z'} (V_c(\vec{b}, z') \eta(\vec{b}, z')) \\
& = -\frac{M_N}{2k^2} \left[\left(2 + b \frac{\partial}{\partial b} \right) V_c(\vec{b}, z) \right] \eta(\vec{b}, z) .
\end{aligned} \tag{8}$$

In the first step, we made use of the fact that the derivative $\partial\eta/\partial z'$ is of higher order to turn the integrand into an exact differential. A similar reasoning, followed by integration by parts, leads to

$$\begin{aligned}
& \frac{M_N}{2k^2} \left(\frac{1}{b} + \frac{\partial}{\partial b} \right) \int_{-\infty}^z dz' (z - z') \frac{\partial V_{so}(\vec{b}, z')}{\partial b} (-ikz') \eta(\vec{b}, z') \\
& = -i \frac{M_N}{2k} \int_{-\infty}^z dz' \left[\left(2 + b \frac{\partial}{\partial b} \right) V_{so}(\vec{b}, z) \right] \eta(\vec{b}, z') ,
\end{aligned} \tag{9}$$

for the Darwin term of Eq. (7). Inserting the expressions of Eqs. (8) and (9), Eq. (6) adopts the form

$$\begin{aligned}
\eta(\vec{b}, z) & = \\
& 1 - i \frac{M_N}{k} \int_{-\infty}^z dz' V_{\text{opt}}(\vec{b}, z') \eta(\vec{b}, z') - \frac{M_N}{2k^2} \left[\left(1 + b \frac{\partial}{\partial b} \right) V_c(\vec{b}, z) \right] \eta(\vec{b}, z) \\
& + \frac{M_N z}{2k^2 b} \left(1 + b \frac{\partial}{\partial b} \right) \int_{-\infty}^z dz' \frac{\partial V_c(\vec{b}, z')}{\partial b} \eta(\vec{b}, z') \\
& + \frac{M_N}{2k^2} V_{so}(\vec{b}, z) (\vec{\sigma} \cdot \vec{b} \times \vec{k} - ikz) \eta(\vec{b}, z) \\
& + \frac{M_N}{2k^2 b} \left(1 + b \frac{\partial}{\partial b} \right) \int_{-\infty}^z dz' (z - z') \left[\frac{\partial}{\partial b} (V_{so}(\vec{b}, z') \vec{\sigma} \cdot \vec{b} \times \vec{k}) \right] \eta(\vec{b}, z') \\
& - i \frac{M_N}{2k} \int_{-\infty}^z dz' \left[\left(2 + b \frac{\partial}{\partial b} \right) V_{so}(\vec{b}, z) \right] \eta(\vec{b}, z') .
\end{aligned} \tag{10}$$

We look for a solution of the form

$$\begin{aligned}
\eta(\vec{b}, z) & = f(\vec{b}, z) \exp \left(-i \frac{M_N}{k} \int_{-\infty}^z dz' V_{\text{opt}}(\vec{b}, z') f(\vec{b}, z') \right) \\
& = f(\vec{b}, z) \exp (i S(\vec{b}, z)) ,
\end{aligned} \tag{11}$$

which should reduce to the ROMEA result of Eq. (5) when terms of higher order than V_{opt}/k are neglected. Accordingly, the function $f(\vec{b}, z)$ should be of the form $f = 1 + O(V_{\text{opt}}/k^2)$. Substituting (11) into Eq. (10) and multiplying by $e^{-iS(\vec{b}, z)}$ yields

$$\begin{aligned}
f(\vec{b}, z) &= 1 - \frac{M_N}{2k^2} \left[\left(1 + b \frac{\partial}{\partial b} \right) V_c(\vec{b}, z) \right] f(\vec{b}, z) \\
&+ \frac{M_N z}{2k^2 b} \left(1 + b \frac{\partial}{\partial b} \right) \int_{-\infty}^z dz' \frac{\partial V_c(\vec{b}, z')}{\partial b} f(\vec{b}, z') \\
&+ \frac{M_N}{2k^2} V_{so}(\vec{b}, z) (\vec{\sigma} \cdot \vec{b} \times \vec{k} - ikz) f(\vec{b}, z) \\
&+ \frac{M_N}{2k^2 b} \left(1 + b \frac{\partial}{\partial b} \right) \int_{-\infty}^z dz' (z - z') \left[\frac{\partial}{\partial b} (V_{so}(\vec{b}, z') \vec{\sigma} \cdot \vec{b} \times \vec{k}) \right] f(\vec{b}, z') \\
&- i \frac{M_N}{2k} \int_{-\infty}^z dz' \left[\left(2 + b \frac{\partial}{\partial b} \right) V_{so}(\vec{b}, z) \right] f(\vec{b}, z'). \tag{12}
\end{aligned}$$

In deriving this equation, we set $e^{iS(\vec{b}, z')} e^{-iS(\vec{b}, z)}$ equal to 1, since higher-order terms are neglected. The difficulty in solving for $f(\vec{b}, z)$ is that Eq. (12) is an integral equation. An expression for $f(\vec{b}, z)$ can, however, be readily obtained by adding $(1 - f)$ terms, which introduce only higher-order terms, to the right-hand side of Eq. (12). This is permitted since we seek for a solution up to order V_{opt}/k^2 . With this manipulation, the function f becomes

$$\begin{aligned}
f(\vec{b}, z) &= 1 - \frac{M_N}{2k^2} \left(1 + b \frac{\partial}{\partial b} \right) V_c(\vec{b}, z) + \frac{M_N z}{2k^2 b} \left(1 + b \frac{\partial}{\partial b} \right) \int_{-\infty}^z dz' \frac{\partial V_c(\vec{b}, z')}{\partial b} \\
&+ \frac{M_N}{2k^2} V_{so}(\vec{b}, z) (\vec{\sigma} \cdot \vec{b} \times \vec{k} - ikz) \\
&+ \frac{M_N}{2k^2 b} \left(1 + b \frac{\partial}{\partial b} \right) \int_{-\infty}^z dz' (z - z') \frac{\partial}{\partial b} (V_{so}(\vec{b}, z') \vec{\sigma} \cdot \vec{b} \times \vec{k}) \\
&- i \frac{M_N}{2k} \int_{-\infty}^z dz' \left(2 + b \frac{\partial}{\partial b} \right) V_{so}(\vec{b}, z). \tag{13}
\end{aligned}$$

The eikonal factor of Eq. (11) with $f(\vec{b}, z)$ given by (13), is a solution of the integral equation (6) to order V_{opt}/k^2 and reduces to the ROMEA result (5) when truncated at order V_{opt}/k . Furthermore, it can be easily verified that the derivative of η is of higher order in V_{opt}/k than η itself. Henceforth, calculations performed with the eikonal factor of Eqs. (11) and (13), are dubbed as the second-order relativistic optical model eikonal approximation (SOROMEA).

3 Results

One way to quantify the overall effect of FSI in $A(e, e'p)$ processes is via the nuclear transparency. The measurements are commonly performed under quasielastic conditions [31–36]. We obtain the theoretical transparencies by adopting similar expressions and cuts as in the experiments. Hence, the nuclear transparency is defined as [37]

$$T = \frac{\sum_{\alpha} \int_{\Delta^3 p_m} d\vec{p}_m S^{\alpha}(\vec{p}_m, E_m, \vec{k})}{c_A \sum_{\alpha} \int_{\Delta^3 p_m} d\vec{p}_m S_{\text{PWIA}}^{\alpha}(\vec{p}_m, E_m)}. \quad (14)$$

Here, S^{α} is the reduced cross section for knockout from the shell α

$$S^{\alpha}(\vec{p}_m, E_m, \vec{k}) = \frac{d^5 \sigma^{\alpha}}{d\Omega_p d\epsilon' d\Omega_{e'}}(e, e'p), \quad (15)$$

where \vec{p}_m and E_m are the missing momentum and energy, K is a kinematical factor and σ_{ep} is the off-shell electron-proton cross section. S_{PWIA}^{α} is the reduced cross section within the plane-wave impulse approximation (PWIA) in the nonrelativistic limit. Further, \sum_{α} extends over all occupied shells α in the target nucleus. The phase-space volume in the missing momentum $\Delta^3 p_m$ is defined by the cut $|p_m| \leq 300$ MeV/c. The A -dependent factor c_A corrects in a phenomenological way for the effect of short-range correlations. We introduce the c_A in the denominator of Eq. (14) because the data have undergone a rescaling with $c_A = 0.9$ (^{12}C) and 0.82 (^{56}Fe).

Transparencies have been computed for the nuclei ^{12}C and ^{56}Fe at planar and constant (\vec{q}, ω) kinematics compatible with the phase space covered in the experiments. For the optical potential, the EDAD1 parametrization of Ref. [38] was used.

In Fig. 1 the ROMEA and SOROMEA results are displayed as a function of the four-momentum transfer Q^2 and compared to the data. Not surprisingly, at high Q^2 , the ROMEA and SOROMEA predictions practically coincide and the role of the second-order eikonal effects grows with decreasing Q^2 . At $Q^2 = 1.7$ (GeV/c) 2 , the ROMEA and SOROMEA transparencies agree to within 1%; while at $Q^2 = 0.3$ (GeV/c) 2 , the difference has risen to 3% for ^{56}Fe and 5% for ^{12}C . The enhancement of the nuclear transparency due to the second-order eikonal corrections is modest, even for values of the four-momentum transfer as low as $Q^2 = 0.2$ (GeV/c) 2 . Both the ROMEA and the SOROMEA predictions tend to slightly underestimate the measurements. The second-order corrections move the predictions somewhat closer to the $Q^2 = 0.34$ (GeV/c) 2 data point.

As the nuclear transparency involves integrations over missing momenta and energies, it may hide subtleties in the theoretical treatment of the FSI mechanisms. Next, we focus on highly exclusive $A(e, e'p)$ quantities and quantify the role of second-order eikonal effects.

An observable that is particularly well suited to study FSI effects is the induced normal polarization

$$P_n = \frac{d^5\sigma(\sigma_n = \uparrow) - d^5\sigma(\sigma_n = \downarrow)}{d^5\sigma(\sigma_n = \uparrow) + d^5\sigma(\sigma_n = \downarrow)}, \quad (16)$$

where σ_n denotes the spin orientation of the ejectile in the direction orthogonal to the reaction plane. Indeed, in the one-photon exchange approximation, P_n vanishes in the absence of FSI.

Fig. 2 shows the missing momentum dependence of the induced normal polarization for the kinematics of Ref. [39], corresponding with $Q^2 \approx 0.5$ (GeV/c)². The calculations are performed with the energy-dependent A -independent (EDAI) potential of Ref. [38]. The ROMEA results are in line with the relativistic distorted-wave impulse approximation (RDWIA) calculations of Ref. [40]. The RDWIA framework was implemented by the Madrid-Sevilla group [41] and relies on a partial-wave expansion of the exact scattering wave function. It is similar to the (SO)ROMEA approach in that both models compute the effect of the FSI with the aid of proton-nucleus optical potentials. Further, the overall agreement with the data is excellent. The second-order eikonal corrections are most pronounced for the $1s_{1/2}$ level. For missing momenta $p_m > 125$ MeV/c, they reduce the magnitude of the P_n for the $1s_{1/2}$ state by roughly 20%, thereby resulting in a marginally better agreement with the highest p_m data point. For $1p_{3/2}$ knockout, on the other hand, the effect of the second-order eikonal corrections is smaller than 5%.

The inclusion of the second-order eikonal effects is particularly visible at high missing momentum, a region where also other mechanisms become important. The qualitative behavior of the meson-exchange and Δ -isobar currents, for instance, is alike [42]. At low missing momenta ($p_m \leq 200$ MeV/c), the induced normal polarization P_n is relatively insensitive to the two-body currents; whereas at higher missing momenta, sizable contributions from the meson-exchange and isobar currents are predicted. The influence of the meson and isobar degrees of freedom is also stronger for knockout from the $1s_{1/2}$ shell than for $1p_{3/2}$ knockout.

In Fig. 2, also calculations neglecting the spin-orbit part $V_{so}(\vec{b}, z) \vec{\sigma} \cdot \vec{b} \times \vec{k}$ are shown. They illustrate that the spin-orbit distortion is the largest source of P_n . Hence, a correct inclusion of this term is essential. Moreover, P_n proves to be rather sensitive to the choice of optical potential [40].

Another $A(e, e'p)$ observable which has been the subject of many investigations is the left-right asymmetry

$$A_{LT} = \frac{d^5\sigma(\phi = 0^\circ) - d^5\sigma(\phi = 180^\circ)}{d^5\sigma(\phi = 0^\circ) + d^5\sigma(\phi = 180^\circ)}. \quad (17)$$

The subscript LT indicates that this quantity is closely related to the longitudinal-transverse response function.

Fig. 3 presents the A_{LT} predictions for the removal of $1p$ -shell protons in ^{16}O in the kinematics of Refs. [43, 44]. The FSI shift the dip in A_{LT} , which is located at $p_m \approx 400$ MeV/c in the relativistic PWIA (RPWIA), to lower values of the missing momentum. This shift is essential to describe the data at $p_m \approx 350$ MeV/c. The exact p_m location and height of the ripple, however, are affected by many ingredients of the calculations, such as the current operator, bound-state wave function, and parametrization of the optical potential [44]. As can be inferred from Fig. 3, the second-order eikonal corrections affect the height, but not the position of the ripple.

We also show the results of our SOROMEA calculations within the so-called noSV approximation. In this approximation, the dynamical enhancement of the lower component of the scattering wave (3) due to the $V_s(r) - V_v(r)$ term is omitted. As such, the SOROMEA-noSV calculations make the same set of assumptions as the EMaf-noSV predictions by the Madrid-Sevilla group. The EMaf-noSV approach is an RDWIA calculation which adopts the EMA in combination with the noSV approximation. The second-order eikonal corrections clearly increase the height of the oscillation in A_{LT} and brings the eikonal noSV calculations in excellent agreement with the corresponding partial-wave prediction EMaf-noSV. Finally, the comparison between the SOROMEA and the SOROMEA-noSV calculations demonstrates that the dynamical enhancement plays a significant role in the description of the A_{LT} data.

In Fig. 4, $^{16}\text{O}(e, e'p)$ cross-section results are displayed for the kinematics of Fig. 3. The spectroscopic factors, which normalize the calculations to the data, were determined by performing a χ^2 fit to the data and are summarized in Table 1. The RDWIA spectroscopic factors are 5–10% higher than the (SO)ROMEA ones. The second-order eikonal corrections hardly affect the values of the extracted spectroscopic factors. Both our (SO)ROMEA calculations and the RDWIA predictions of the Madrid-Sevilla group do a very good job of representing the data over the entire p_m range. For missing momenta $|p_m| \leq 250$ MeV/c, the (SO)ROMEA and RDWIA results are in excellent agreement. The impact of the second-order eikonal corrections on the computed differential cross sections is almost negligible for p_m below the Fermi momentum, but can be as large as 30% at high p_m . The inclusion of the second-order effects improves the agreement with the RDWIA calculations at

these high missing momenta. Results for the effective response functions R_L , R_T , R_{LT} , and R_{TT} are not shown, but the effect of the second-order eikonal corrections is similar to the effect on the differential cross section.

	RPWIA	ROMEIA	SOROMEIA	RDWIA
$1p_{3/2}$	0.55	0.84	0.83	0.92
$1p_{1/2}$	0.47	0.75	0.74	0.78

Table 1

The spectroscopic factors for the $^{16}\text{O}(e, e'p)$ reaction of Ref. [43], as obtained with a χ^2 procedure.

4 Conclusions

We have developed a formalism to account for second-order corrections in the eikonal approximation. Our model is relativistic and includes both the central and spin-orbit parts of the optical potentials. The formalism has been applied to $A(e, e'p)$ processes. Our numerical calculations show that the effect of the second-order eikonal corrections on $A(e, e'p)$ observables is rather limited for $Q^2 \geq 0.2$ (GeV/c) 2 . The nuclear transparency calculations confirm the expected energy dependence of the eikonal corrections: the effect decreases with increasing Q^2 . Concerning the p_m dependence of the $A(e, e'p)$ observables, the effect of the second-order eikonal corrections is minor except at high missing momenta. In this high- p_m region, the eikonal corrections affect the observables up to an order of 30%, thereby bringing the calculations closer to the data and/or the RDWIA calculations. The robustness of the first-order eikonal approximation, which emerges from this study, can be invoked to explain the success of the Glauber approach to $A(e, e'p)$ down to relatively low kinetic energies of 200 MeV.

Acknowledgements

This work was supported by the Fund for Scientific Research, Flanders (FWO).

References

- [1] G.P. McCauley, G.E. Brown, Proc. Phys. Soc. London 71 (1958) 893.
- [2] R.J. Glauber, in: W.E. Brittin, et al. (Eds.), Lectures in Theoretical Physics, Interscience, New York, 1959.

- [3] C.J. Joachain, *Quantum Collision Theory* (Elsevier, Amsterdam, 1975).
- [4] W.R. Greenberg, G.A. Miller, Phys. Rev. C 49 (1994) 2747.
- [5] A. Bianconi, M. Radici, Phys. Lett. B 363 (1995) 24.
- [6] H. Ito, S.E. Koonin, R. Seki, Phys. Rev. C 56 (1997) 3231.
- [7] D. Debruyne, J. Ryckebusch, W. Van Nespén, S. Janssen, Phys. Rev. C 62 (2000) 024611.
- [8] L.L. Frankfurt, E. Moniz, M. Sargsyan, M.I. Strikman, Phys. Rev. C 51 (1995) 3435.
- [9] N.N. Nikolaev, A. Szcurek, J. Speth, J. Wambach, B.G. Zakharov, V.R. Zoller, Nucl. Phys. A 582 (1995) 665.
- [10] S. Jeschonnek, T.W. Donnelly, Phys. Rev. C 59 (1999) 2676.
- [11] A. Kohama, K. Yazaki, R. Seki, Nucl. Phys. A 662 (2000) 175.
- [12] O. Benhar, N. Nikolaev, J. Speth, A. Usmani, B. Zakharov, Nucl. Phys. A 673 (2000) 241.
- [13] C. Ciofi degli Atti, L.P. Kaptari, D. Treleani, Phys. Rev. C 63 (2001) 044601.
- [14] M. Petraki, E. Mavrommatis, O. Benhar, J.W. Clark, A. Fabrocini, S. Fantoni, Phys. Rev. C 67 (2003) 014605.
- [15] J. Ryckebusch, D. Debruyne, P. Lava, S. Janssen, B. Van Overmeire, T. Van Cauteren, Nucl. Phys. A 728 (2003) 226.
- [16] S.J. Wallace, Phys. Rev. Lett. 27 (1971) 622;
S.J. Wallace, Ann. Phys. (N.Y.) 78 (1973) 190;
S.J. Wallace, Phys. Rev. D 8 (1973) 1846;
S.J. Wallace, J.A. McNeil, Phys. Rev. D 16 (1977) 3565;
S.J. Wallace, Phys. Rev. C 29 (1984) 956.
- [17] D. Waxman, C. Wilkin, J.-F. Germond, R.J. Lombard, Phys. Rev. C 24 (1981) 578.
- [18] G. Fäldt, A. Ingemarsson, J. Mahalanabis, Phys. Rev. C 46 (1992) 1974.
- [19] F. Carstoiu, R.J. Lombard, Phys. Rev. C 48 (1993) 830.
- [20] M.H. Cha, Y.J. Kim, Phys. Rev. C 51 (1995) 212.
- [21] J.S. Al-Khalili, J.A. Tostevin, J.M. Brooke, Phys. Rev. C 55 (1997) R1018.
- [22] C.E. Aguiar, F. Zardi, A. Vitturi, Phys. Rev. C 56 (1997) 1511.
- [23] J.A. Tjon, S.J. Wallace, Phys. Rev. C 74 (2006) 064602.
- [24] A. Baker, Phys. Rev. D 6 (1972) 3462.

- [25] J.J. Kelly, *Adv. Nucl. Phys.* 23 (1996) 75.
- [26] B.D. Serot, J.D. Walecka, *Adv. Nucl. Phys.* 16 (1986) 1.
- [27] R.J. Furnstahl, B.D. Serot, H.-B. Tang, *Nucl. Phys. A* 615 (1997) 441.
- [28] T. de Forest, *Nucl. Phys. A* 392 (1983) 232.
- [29] R.D. Amado, J. Piekarewicz, D.A. Sparrow, J.A. McNeil, *Phys. Rev. C* 28 (1983) 1663.
- [30] J.J. Kelly, *Phys. Rev. C* 60 (1999) 044609.
- [31] G. Garino, et al., *Phys. Rev. C* 45 (1992) 780.
- [32] T.G. O'Neill, et al., *Phys. Lett. B* 351 (1995) 87.
- [33] N.C.R. Makins, et al., *Phys. Rev. Lett.* 72 (1994) 1986.
- [34] D. Abbott, et al., *Phys. Rev. Lett.* 80 (1998) 5072.
- [35] D. Dutta, et al., *Phys. Rev. C* 68 (2003) 064603.
- [36] D. Rohe, et al., *Phys. Rev. C* 72 (2005) 054602.
- [37] P. Lava, M.C. Martínez, J. Ryckebusch, J.A. Caballero, J.M. Udías, *Phys. Lett. B* 595 (2004) 177.
- [38] E.D. Cooper, S. Hama, B.C. Clark, R.L. Mercer, *Phys. Rev. C* 47 (1993) 297.
- [39] R.J. Woo, et al., *Phys. Rev. Lett.* 80 (1998) 456.
- [40] J.M. Udías, J.R. Vignote, *Phys. Rev. C* 62 (2000) 034302.
- [41] J.M. Udías, P. Sarriguren, E. Moya de Guerra, E. Garrido, J. A. Caballero, *Phys. Rev. C* 48 (1993) 2731.
- [42] J. Ryckebusch, D. Debruyne, W. Van Nespén, S. Janssen, *Phys. Rev. C* 60 (1999) 034604.
- [43] J. Gao, et al., *Phys. Rev. Lett.* 84 (2000) 3265.
- [44] K.G. Fissum, et al., *Phys. Rev. C* 70 (2004) 034606.

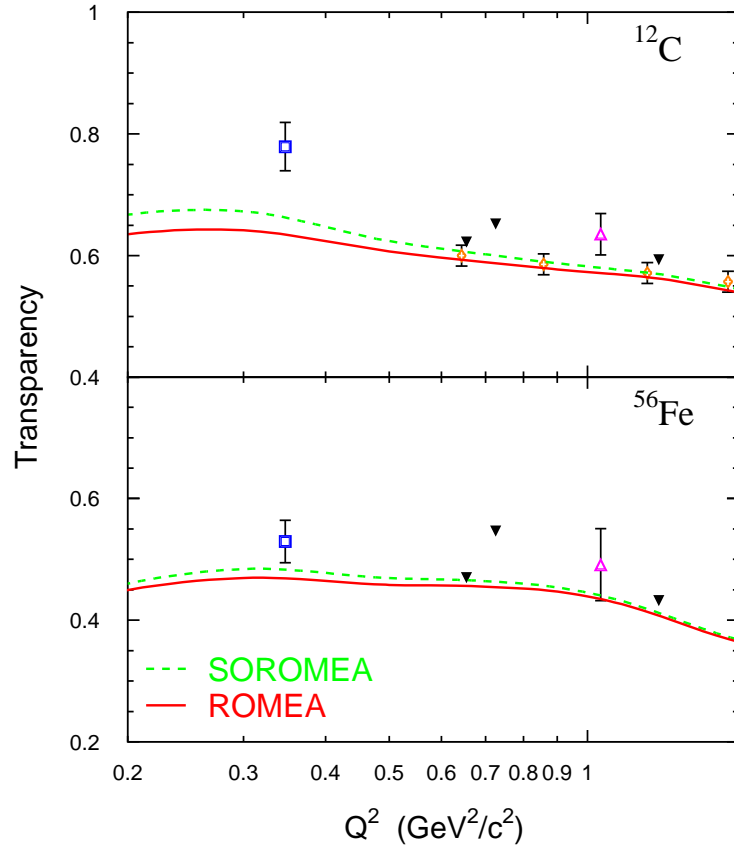


Fig. 1. Nuclear transparencies versus Q^2 for $A(e, e'p)$ reactions in quasielastic kinematics. The SOROMEA (dashed lines) are compared to the ROMEA (solid lines) results. The EDAD1 potential [38] has been employed in both formalisms. Data points are from Refs. [31] (open squares), [32, 33] (open triangles), [34, 35] (solid triangles), and [36] (open diamonds).

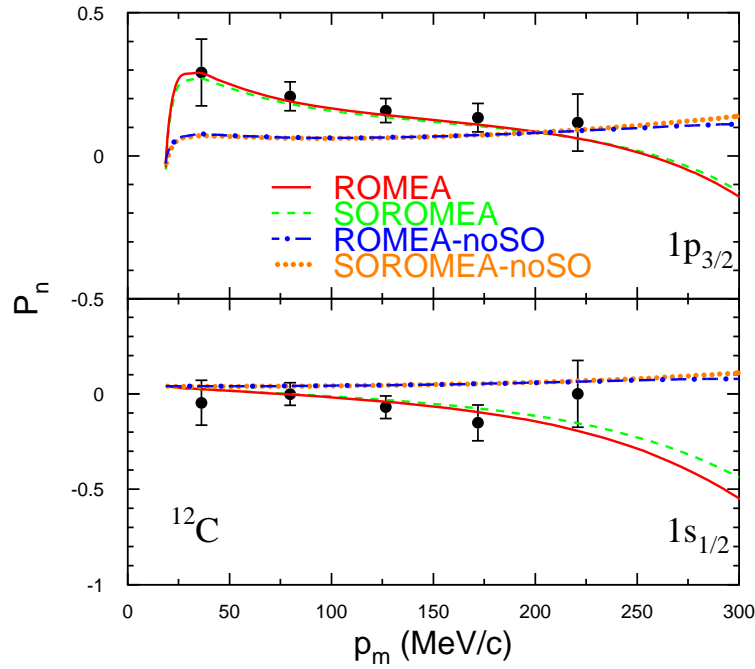


Fig. 2. Induced normal polarization P_n for proton knockout from the $1p_{3/2}$ (upper panel) and $1s_{1/2}$ (lower panel) shell in the $^{12}\text{C}(e, e'\vec{p})$ reaction. The kinematics is determined by beam energy $\epsilon = 579$ MeV, momentum transfer $q = 760$ MeV/c, energy transfer $\omega = 292$ MeV, and azimuthal angle $\phi = 180^\circ$. The solid (dashed) curves represent ROMEA (SOROMEA) calculations. The dot-dashed (dotted) curves refer to predictions obtained within the ROMEA (SOROMEA) frameworks, with the spin-orbit term $V_{so}(\vec{b}, z) \vec{\sigma} \cdot \vec{b} \times \vec{k}$ turned off. The data are from Ref. [39].

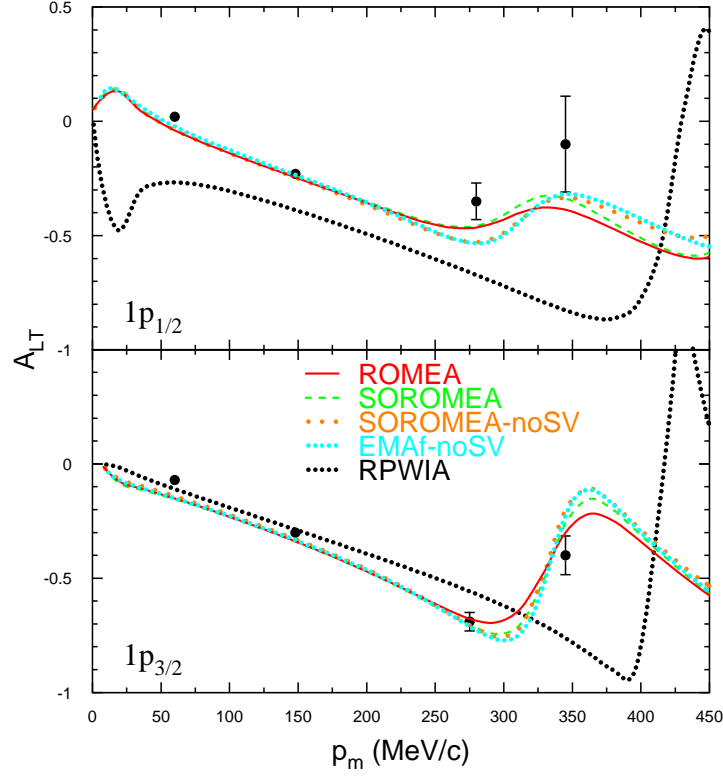


Fig. 3. The left-right asymmetry A_{LT} for the $^{16}\text{O}(e, e'p)$ experiment of [43]. The kinematics was $\epsilon = 2.442$ GeV, $q = 1$ GeV/c, and $\omega = 445$ MeV (i.e., $Q^2 = 0.8$ (GeV/c) 2). The red solid (green dashed) lines show the results of the ROMEA (SOROMEA) calculations. The SOROMEA-noSV (orange long-dotted curves) calculations differ from the SOROMEA calculations in that the dynamical enhancement of the lower component of the scattering wave function is neglected. The cyan short-dotted curves present the results from an RDWIA calculation where the spinor distortions in the scattered wave are neglected. All calculations use the EDAI version for the optical potentials [38]. The black short-dotted curves represent the RPWIA results. The data points are from Ref. [43].

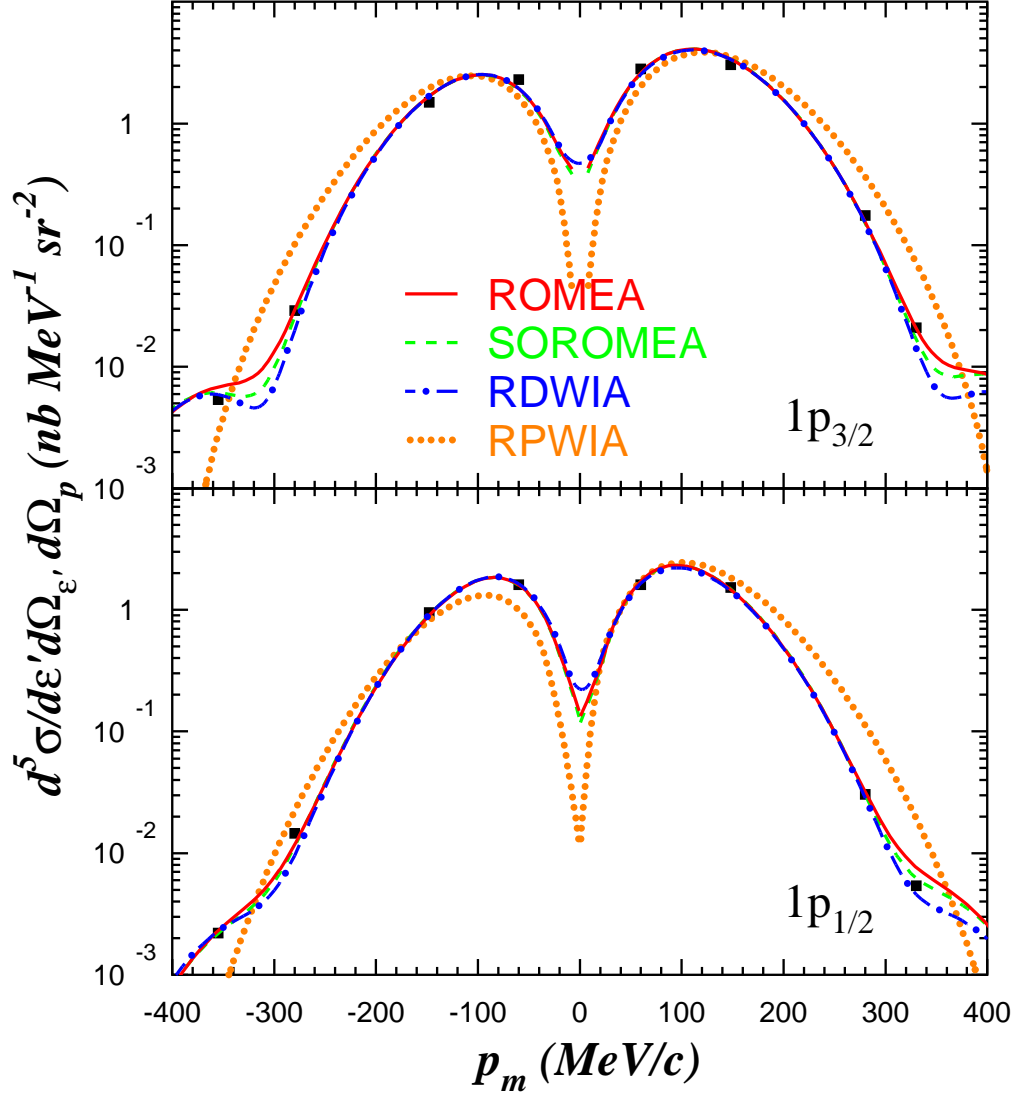


Fig. 4. $^{16}\text{O}(e, e'p)$ cross sections compared to ROMEA, SOROMEA, RDWIA, and RPWIA calculations for the constant (\vec{q}, ω) kinematics of Fig. 3. The calculations use the optical potential EDAI [38]. The data are from Ref. [43] and the RDWIA results from Ref. [44]. The following convention is adopted: positive (negative) p_m corresponds to $\phi = 180^\circ$ ($\phi = 0^\circ$).